

COMPUTER-AIDED ANALYSIS OF EDDY CURRENT ROTATING PROBE DATA*

S. Bakhtiari, J. Y. Park, D. S. Kupperman, and W. J. Shack
Argonne National Laboratory
Energy Technology Division
9700 South Cass Avenue
Argonne, Illinois 60439
E-mail: bakhtiari@anl.gov

The submitted manuscript has been created by the University of Chicago as Operator of Argonne National Laboratory under Contract No. W-31-109-ENG-38 with the U.S. Department of Energy. The U.S. Government retains for itself, and others acting on its behalf, a paid-up, nonexclusive, irrevocable worldwide license in said article to reproduce, prepared derivative works, distribute copies to the public, and perform publicly and display publicly, by or on behalf of the Government.

To be published in the Proceedings of the 4th CNS International Steam Generator Conference, May 5-8, 2002, Toronto, Canada.

* Work sponsored by the Office of Nuclear Regulatory Research, U.S. Nuclear Regulatory Commission, under Job Code W6487.

COMPUTER-AIDED ANALYSIS OF EDDY CURRENT ROTATING PROBE DATA

S. Bakhtiari, J. Y. Park, D. S. Kupperman, and W. J. Shack

ABSTRACT

Eddy current (EC) estimate of flaw size obtained from inservice inspection is often the primary means of assessing the structural integrity of steam generator tubes. Reliable prediction of failure pressure and leak rate in tubes with complex cracking requires more detailed information about the geometry and extent of degradation than is generally available from conventional bobbin coil examinations. High-resolution inspections with EC rotating probes are thus carried out on selected regions of tubing to provide the more extensive nondestructive evaluation (NDE) information that is needed to better assess flaw size and distribution. Interpretation of signals from complex cracking that are often distorted by coherent and incoherent noise can be a challenging NDE task. Studies at Argonne National Laboratory have demonstrated that computer-aided data analysis can be used for more accurate and efficient processing of the large amounts of data collected by such probes. The basic structure of a rule-based multiparameter data analysis algorithm is described in this paper. Multiple-frequency inspection data from a standard rotating pancake coil were used for the analyses. The codes were implemented as MATLAB scripts and provide, as the final outcome, profiles of flaw depth in a section of tube. Graphical user interface tools were devised to read the information needed to carry out various stages of data processing. These interactive tools allow conversion, calibration, analysis, and display of data in various formats. Representative cases of estimated flaw profiles are shown for tube specimens with laboratory-grown cracks (with and without simulated artifacts) that were used to assess sizing accuracy. The statistical analyses used to determine NDE performance are also discussed briefly. Results of investigations to date suggest that improved resolution and sizing accuracy can be obtained in a fraction of the time required for manual analysis.

Argonne National Laboratory
Energy Technology Division
9700 South Cass Avenue
Argonne, Illinois 60439
E-mail: bakhtiari@anl.gov

COMPUTER-AIDED ANALYSIS OF EDDY CURRENT ROTATING PROBE DATA

S. Bakhtiari, J. Y. Park, D. S. Kupperman, and W. J. Shack

1. INTRODUCTION

The basic structure of a computer-aided data analysis algorithm that was implemented to more accurately and efficiently process eddy current (EC) rotating probe data is described. Some key objectives of this work have been to characterize flaws in the Argonne National Laboratory (ANL) tube bundle mock-up in order to minimize the expense of tedious destructive examinations and to further assist parallel studies under this program on prediction of tube structural integrity from nondestructive evaluation (NDE) estimates of flaw profiles. Initially, implementation of data conversion and calibration routines for off-line manipulation of EC data is addressed. A general description of signal processing and data analysis schemes adapted for manipulation of C-scan recordings with high-resolution rotating probes is presented. Test cases selected from analyses of laboratory-produced specimens with chemically induced cracks are provided to illustrate the NDE results. Also included are representative cases that compare flaw profiles estimated by NDE with the true state as determined by fractography. Statistical analyses carried out to determine the significance of NDE uncertainties in predicting the structural integrity of tubing are briefly discussed. NDE assessments have been limited to analyses of data from rotating pancake coils; however, many of the fundamental processes for computer-aided data analysis are applicable to other probe geometries and coil configurations.

2. COMPUTER-AIDED ANALYSIS OF EDDY CURRENT INSPECTION DATA

Manual analysis of multiple-frequency EC data is a tedious and challenging process. No qualified technique, manual or automated, currently exists that could provide a reliable estimate of flaw size over a wide range of steam generator (SG) tubing damage. Conventional data analysis methods become rather subjective when dealing with complex forms of degradation such as stress corrosion cracking (SCC). Signal distortion by interference from internal/external artifacts near a flaw further complicates discrimination of flaw signals from noise. In comparison to high-speed bobbin coil inspections, high-resolution multicoil rotating and array probes generate enormous amounts of data over comparable scanning lengths. Rotating probe inservice inspection (ISI) of SG tubing is, thus, generally restricted to areas that are historically predisposed to known damage mechanisms and sections of particular interest that are flagged by initial bobbin coil examinations. More extensive application of such probes to improve NDE reliability rests, in part, on automating various stages of the data screening process. Computer-aided data analysis is a viable means to overcome many of the challenges associated with reliable processing of data acquired with high-resolution probes.

2.1 Data Processing Structure

Figure 1 depicts the basic structure of the algorithm that was implemented to allow for off-line analysis of data acquired with a commercial EC testing instrument; in the figure, blocks associated with the processes mentioned here are numbered. Output of the acquisition block shown in Fig. 1 consists of the digitized recordings of a multiple-frequency inspection system. The EC testing instrumentation and software currently in use at ANL is a Miz-30™ (Zetec, Inc.) remote data acquisition unit that is controlled under the HP-UX-based Eddynet™ (Zetec, Inc.) environment. To facilitate development of algorithms for evaluation of EC inspection results, codes have been implemented to convert the raw inspection data to a standard file format. All data analysis and signal processing algorithms have been implemented by using the PC-based software MATLAB, which is a high-level scripting language that provides an efficient environment for developing codes, together with convenient graphical user interfaces (GUIs) and graphical displays of the results.

The block diagram shown in Fig. 1 can be divided into three basic components: data conversion, calibration, and analysis stage. Each block is described in the following sections. In the conversion stage (Block 1), digitized recordings of inspection data that sequentially represent in-phase and quadrature signal components are converted to a readable format for off-line manipulation. In the subsequent stage, multiple-frequency raw EC data, shown as Block 2, are calibrated for all of the recorded frequency channels. Finally, in the data analysis stage, represented by Blocks 3-6, calibrated data are processed to ultimately produce NDE profiles that represent sizing estimates along a selected test section of a tube.

2.2 Conversion and Calibration Routines

A series of algorithms has been implemented under the MATLAB environment to carry out the conversion, normalization, and reformatting of EC readings for subsequent analysis. An interactive MATLAB script calls the data retrieval and calibration routines through a single GUI control window. The data conversion routine extracts the essential header information, such as the number of channels and their associated frequencies, from the original Eddynet-formatted files. The decoded header information contains the frequency and channel configuration that is subsequently used to sort out raw EC readings. The reformatted data matrix, along with the header and coil configuration information, is then stored in a user-defined data file. Normalization values of all the available channels are calculated by using the inspection results from a calibration standard tube. These values consist of amplitude scaling factors, phase angle rotations, and null values, the automatic calculation of which is based on user-defined approximate locations of known indications on the tube. Finally, raw EC recordings are calibrated by another code that is also activated from the main menu and applies the previously calculated normalization factors to each new raw data file [1,2].

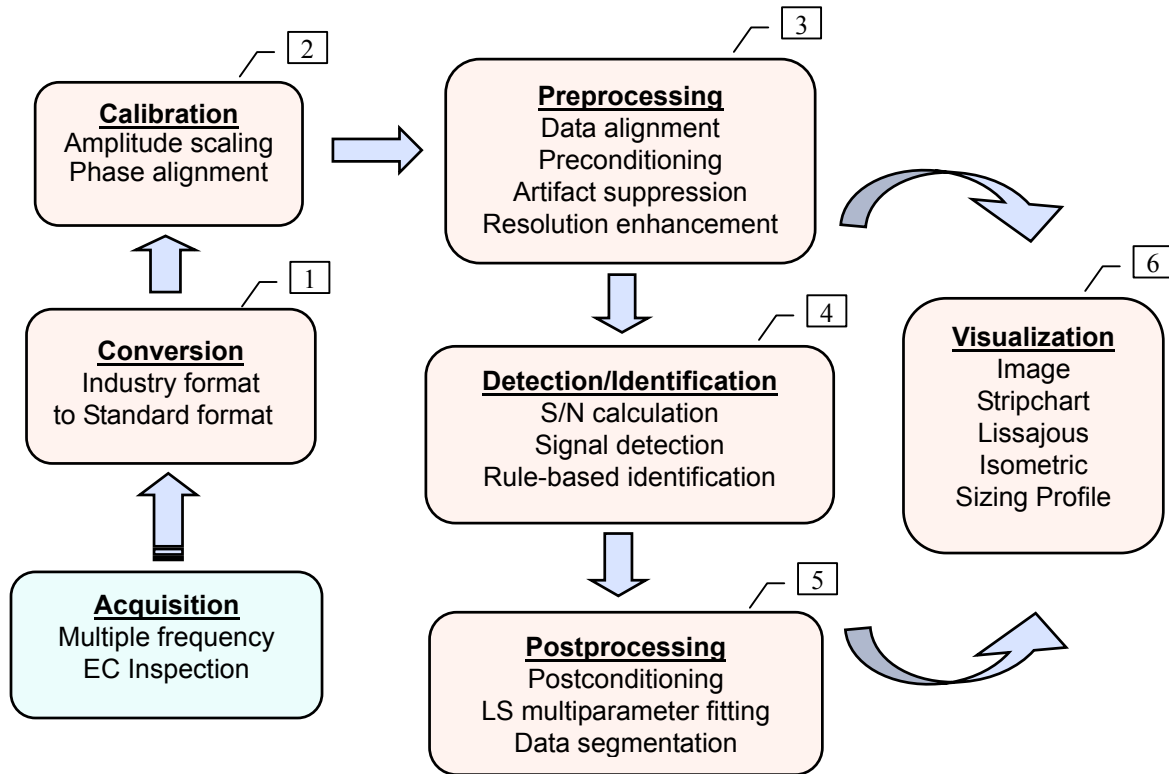


Figure 1. Schematic diagram showing basic structure of computer-aided data analysis algorithm. Blocks associated with operations described in this report are numbered.

Calibration of raw EC data plays an important role in any data analysis procedure. Conventional phase angle calibration procedures for normalizing EC data are carried out manually, and routinely involve visual alignment of the impedance-plane signal trajectory (i.e., lissajous plot) with respect to some reference indication. This implies that the extent of background fluctuations and signal-to-noise (S/N) ratio, as well as analyst judgment, could affect the calibration process and consequently lead to varying estimates of a desired parameter. Because estimates of flaw depth from phase angle information of multifrequency inspection data depend heavily on initial calibrations, it is expected that computer-aided data calibration routines will play an essential role in uniform and accurate normalization of raw EC data.

2.3 Signal Processing, Data Analysis, and Display Routines

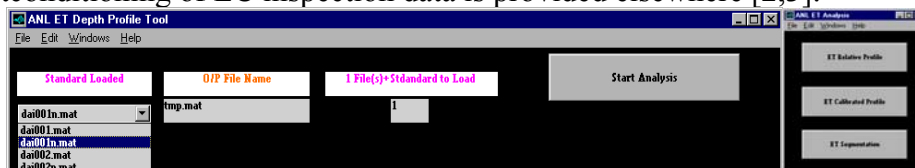
In Fig. 1, the data analysis section (Blocks 3-6) is composed of three basic stages: preprocessing, flaw detection and identification, and postprocessing of data. These blocks consist of various scripts that successively perform the calculation of S/N ratio for all channels, apply filters for pre- and postprocessing of data, and ultimately combine multiple-frequency information from all processed channels to provide an estimate of the depth profile for the entire tubing test section. Both frequency- and spatial-domain filters are incorporated for signal conditioning, baseline reduction, and resolution enhancement. Initially, the S/N ratio is calculated from a user-defined approximate location along the trace baseline and the minimum detectable amplitude from a calibration standard tube. Subsequently, this information is used to implement a series of filters

that suppress artifacts and baseline fluctuations, and enhance or restore signals. Filter characteristics are determined by taking into account both the coil configuration and the sampling frequency of the inspection data. Flaws and their origin are identified by a series of rules that are applied to the multiple-frequency EC data. Both amplitude and phase relationships among the processed channels are used at this stage of the process. Finally, the phase information at multiple frequencies is combined to calculate the depth profile for the tube test section in reference to known indications on a calibration standard tube.

A series of algorithms has been implemented as MATLAB scripts to provide profiles of flaw depth in a SG tube test section from NDE inspection results. These codes are executed through a user interface tool to automatically process EC inspection results acquired with rotating probes at multiple frequencies. Figure 2 shows the main window of the GUI tool, which incorporates various algorithms for processing raw EC data. Pull-down menus, push buttons, and editable text areas on the display can be activated to perform the various stages of the data analysis process. Figure 2 also shows several forms of graphics that are currently in place to visualize data at various stages of analysis. Subsequent to depth profile calculations, estimated values are converted to percent of tube wall thickness. Reconstruction of helically scanned data into C-scan format allows the observation of sizing results from any azimuth and elevation view angle and for any axial or circumferential cross section of the tube. Scaling of data in axial and circumferential directions allows direct deduction of flaw extent along the tube.

2.3.1 Application of Digital Filters

For processing of eddy current NDE data, digital filters generally serve three basic purposes: noise reduction, artifact suppression, and signal enhancement or restoration. All of these operations, however, are fundamentally aimed at improving the S/N ratio. In this context, noise is characteristically defined as any unwanted signal, regardless of its source. Frequency- and spatial-domain transformations are widespread in signal and data processing applications. In general, they provide information that may not readily be available in the original domain. When frequency-domain filtering is the desired method, data are transformed to the Fourier domain, processed, and then reverse-transformed into the original domain. The choice for using either a frequency- or spatial-domain operation depends on the signal features that must be suppressed or preserved. No strict rules can be given for the use of spatial- or frequency-domain filtering. For EC signals, frequency-domain operations are often better suited for reducing low-frequency baseline fluctuations and high-frequency noise. Spatial-domain filtering, on the other hand, is typically more appropriate for enhancing subtle features in the data. In general, when the frequency content of the signal and noise are well separated, frequency-domain operations are the preferred method for noise suppression. A more detailed description of digital filters for pre- and postconditioning of EC inspection data is provided elsewhere [2,3].



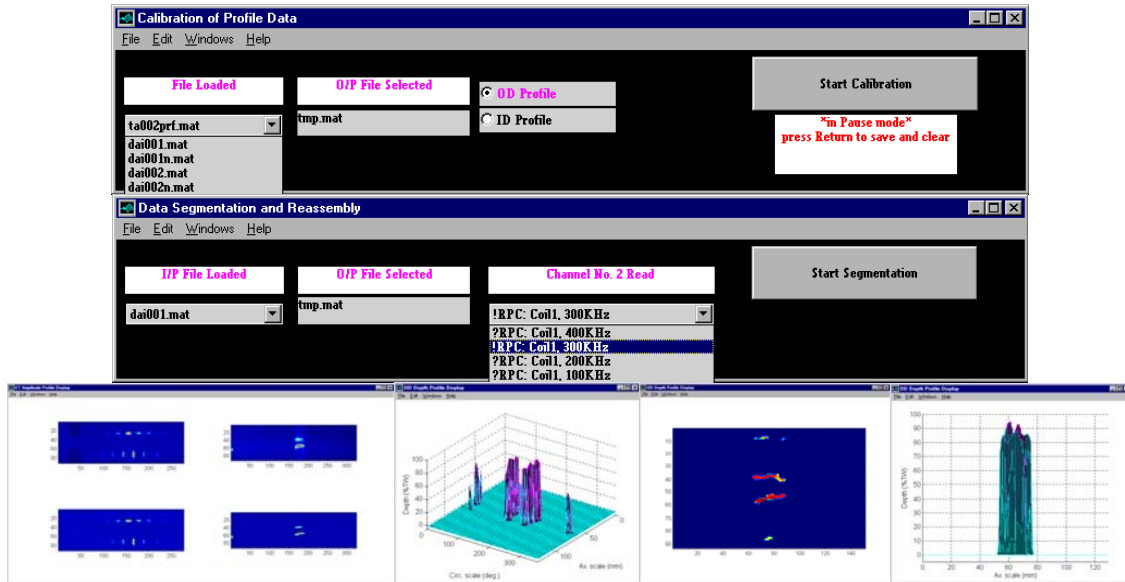


Figure 2. Series of MATLAB-based graphical user interface (GUI) tools (top three rows) for automated analysis of EC inspection results acquired with standard commercial instruments. Also shown (bottom row) are several graphical display formats, such as image, terrain, and cross-sectional NDE profiles of tube test sections, at various stages of analysis.

2.3.2 Signal Enhancement and Restoration

Two basic approaches for improving data quality are the signal enhancement and signal restoration methods. Signal enhancement refines the quality of data without any knowledge of the degradation phenomenon. Signal restoration, on the other hand, is founded on the assumption that the degradation source is well understood so that an inverse process could be implemented to recover the true response. The principal objective in both cases is to treat the data so the result is more suited for a specific application than the original data. Although the two approaches are clearly differentiated in most standard data processing applications, distinction between the two becomes less apparent in practical applications associated with the EC testing of SG tubing. This is because of the difficulty to accurately model the underlying degradation phenomenon that arises from the combined influence of many factors, in addition to the blurring effect of the coil impulse response. Both data enhancement and approximate restoration schemes have been incorporated into the multiparameter data analysis algorithm. Studies to date suggest that comparable results can be achieved by the two techniques for processing EC rotating probe data. Signal restoration, referred to here as approximate deconvolution or inverse filtering, is implemented in the frequency domain. Signal enhancement, on the other hand, is implemented directly in the original spatial domain. Although deconvolution-based methods are generally expected to produce more accurate results, they are also computationally more intensive.

The application of approximate deconvolution schemes to real-time processing of multifrequency inspection results has been investigated at ANL [2,3] in a study that was prompted by the need for more accurate characterization of complex cracking morphologies in SG tubing. Deconvolution techniques are used in a wide range of signal processing applications,

primarily to recover signals distorted by the sensing environment. In EC inspection applications, pseudoinverse filters could be effective for enhancement of spatial resolution that is degraded by the finite spread of the coil-induced field. Better separation of flaw indications from extraneous signals could, in turn, improve the estimation of flaw depth determined from the phase-angle information of multifrequency data. Frequency-dependent signal restoration could also help reduce differences in probe response at various frequencies.

When the exact form of the degradation process can only be approximated, signal enhancement techniques are often the first choice for the treatment of data. Because such techniques can be implemented directly in the original domain, they are computationally efficient. Signal enhancement is achieved by applying prestored kernels to the EC C-scan. Both smoothing and peak restoration are attained in this manner. As an alternative approach to the frequency-domain signal restoration techniques, polynomial fitting based on the method of least-squares (LS) can be implemented to effectively carry out such basic operations as smoothing and peak detection directly in the spatial domain. Primary advantages of this method in comparison to frequency domain methods noted earlier are ease of implementation and processing speed. Polynomial fitting can be performed as a one-step convolution operation in the spatial domain. Convolution kernels in this case are pre-stored coefficients and weights (normalization factors) that are calculated by the LS method. Symmetric kernels are used to ensure that the location of the signal peak is not shifted. Two major restrictions for reliable application of this method are the uniformity of the digitization rate and continuity of the data. For EC inspection results, it may be necessary to resample data off-line when the digitization rates in axial and circumferential directions deviate from each other.

Eddy current readings on a collection of 22.2-mm (0.875-in.)-diameter Alloy 600 tubes with laboratory-produced cracking were analyzed by the multiparameter data analysis scheme described in this report. Flaws in this small set of samples consisted primarily of OD axial cracking in free-span regions, and circumferential cracking in roll-transition regions, plus a single specimen with axial ID cracking at a dented tube support plate (TSP). Multiple-frequency NDE data used in this study were acquired with a standard three-coil rotating probe that contained a 2.92-mm (0.115-in.) pancake, a midrange +Point™, and a 2.03-mm (0.080-in.) high-frequency pancake coil. The primary pancake coil readings were utilized for the analyses. The calibration standard contained 18 axially and circumferentially orientated EDM notches that originated from the OD and ID of the tube and ranged in depth from 20 to 100% throughwall (TW). All notches were 6.35 mm (0.25 in.) long.

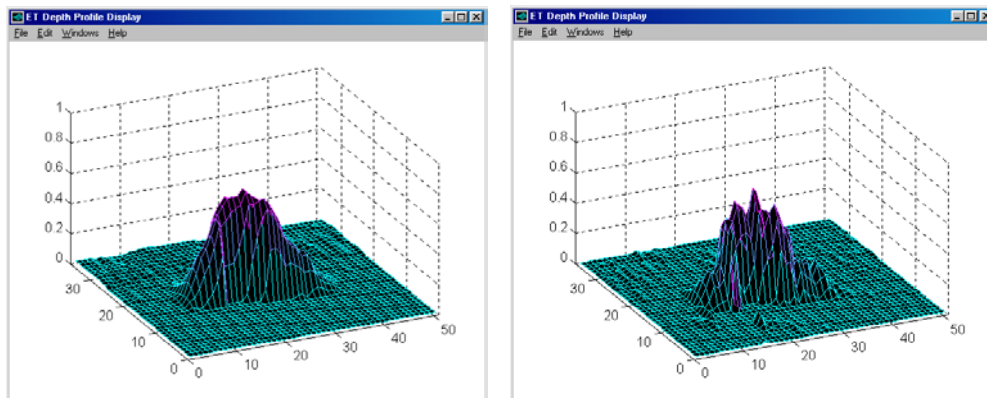
Figure 3 shows the normalized depth profile of specimens with laboratory-grown, longitudinal ODSCC. For both test cases, only the portion of tube near the flaw is displayed. In reference to the calibration standard, the maximum flaw depth estimate in the laboratory-produced specimen was ≈80% TW. Figures 3(a) and (b) display, respectively, the estimated two-dimensional profiles of the flawed segment without and with application of the deconvolution process. Unlike the gradual tapering of the flaw depth seen in Fig. 3(a), the restored profile in Fig. 3(b) shows that the depth of the flaw is rather uniform in the center, with a sharp drop at the two ends of the crack. Similar results are shown in Figs. 3(c) and (d) for another laboratory-produced specimen with ODSCC degradation.

The fundamental limitation of data enhancement and restoration techniques for the processing of EC signals could be attributed to the flow of current in a conducting medium that is governed by the diffusion phenomenon. This limitation suggests that distortion is not simply a modulation of signal amplitude. Instead, the waveform could experience a complete alteration of structure that is not linearly dependent on its original form. Another factor that could significantly influence the degree to which a signal can be recovered is the lack of separation between the spectral content of flaw indications and extraneous signals. Internal/external artifacts and design discontinuities (e.g., conducting and magnetic deposits, tube dimensional variations, and external support structures) could produce signal trajectories with spectral components that are close to those from flaw indications. Furthermore, practical sampling rates that are typically used to acquire ISI data with rotating probes do not render the continuous smooth signals that are essential for optimal restoration by inverse-filtering schemes. Finally, it is important to note that physically realizable optimal inverse filters are often unstable. For this reason, approximate deconvolution algorithms may provide the best alternative for real-time restoration of EC flaw signals for practical ISI applications.

2.3.3 Multiparameter Data Analysis

Multivariate data analysis techniques are the foundation of various operations in the processing of EC data. Both regression and factor-based techniques fit into this category of data manipulation. More prominent areas of application to EC ISI data are in algorithms used to suppress unwanted signals and in predictive models that attempt to correlate NDE parameters to single or multiple independent variables, such as flaw size or tube structural integrity. Three separate algorithms were investigated and have been adapted for use in various areas of research associated with the EC testing of SG tubing: multiple linear regression (MLR), principal component regression (PCR), and partial least squares (PLS) techniques. Conventional LS-based regression has been used primarily in standard artifact suppression schemes, commonly referred to as mixing algorithms. The more versatile PLS algorithm has been used in a wider range of applications, including more sophisticated mixed suppression schemes and predictive models [2,3].

Multivariate analysis is also used in the final stage of data analysis (shown in Block 5 of Fig. 1) to estimate the depth profile of a test section. Processed data from multiple channels is simultaneously used to construct a model that correlates the NDE results to flaw size and origin.



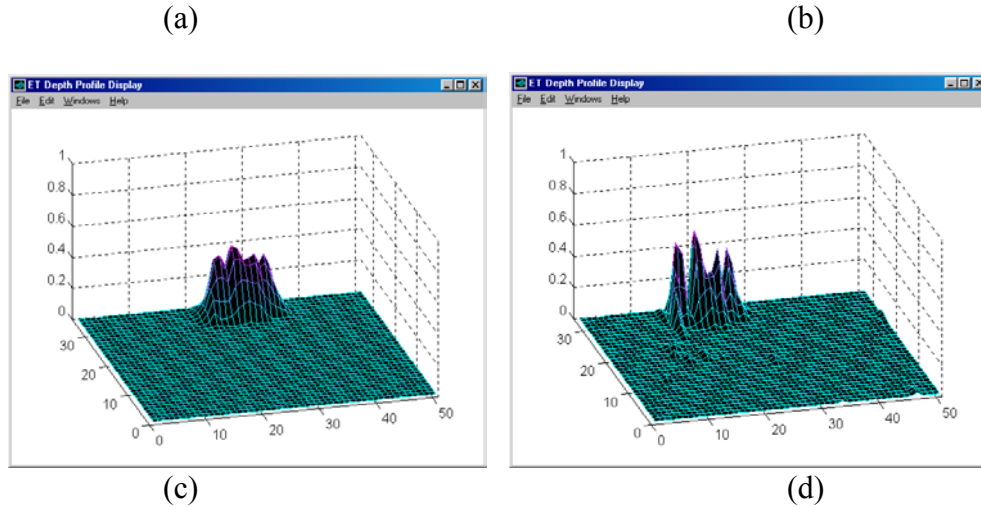


Figure 3. Data analysis results for specimens with laboratory-grown, longitudinal ODSCC showing terrain plot of (a,c) relative OD depth profile for cracked zone and (b,d) profile restored by inverse filtering. Maximum crack depths are estimated to be $\approx 80\%$ TW (top) and $>80\%$ TW (bottom), respectively. Isometric display of results shows finer details in restored profiles.

The reliability of any predictive correlation depends heavily on the calibration data used to construct that model. Both the range and composition of training data play crucial roles. In regard to the analysis of EC data, information is thus needed on a wide range of flaw sizes and types in the calibration standard tube. In addition, a useful set of test frequencies is of utmost importance.

2.3.4 Rule-Based Flaw Identification

As in the manual analysis of EC inspection data, the characteristic behavior of EC signals as a function of frequency can be utilized in computer-aided data analysis algorithms. Because all available information is indiscriminately examined, such algorithms allow more effective identification of subtle forms of degradation. Identification of flaws and their origin is performed by applying a series of rules to the preprocessed multiple-frequency EC data. This intermediate stage of data analysis is shown in Block 4 of Fig. 1. Rules are coded as a series of conditional statements (i.e., IF-THEN) that are sequentially applied to the selected data segments. Calculation of S/N ratio from the earlier stages of the analysis is used to set the minimum threshold for sorting signals that are to be examined. Combined amplitude and phase-based rules are implemented to better discriminate between potential flaws and noise. Rules that are currently in place are set to be generally conservative to identify flawed regions of SG tubes. As a tradeoff between conservatism and sensitivity, they can be adjusted to some degree based on the value of the S/N ratio for a particular test section. The current set of rules is fixed for a specific coil configuration and frequency range. Future studies in this area should focus on semiautomated implementation of rules to more effectively deal with the expected variability in coil design and ISI data acquisition procedures.

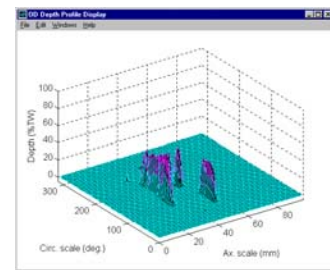
2.4 Assessment of Sizing Accuracy in Presence of Artifacts

To assess the effect of various artifacts on flaw signals, results from the analyses of a subset of laboratory-produced specimens were examined. Data were collected on these tubes with and without the removable collars that simulate artifacts such as TSP, sludge, magnetite, and copper deposits that may be present to various degrees during field inspections. Representative test cases are displayed as amplitude images of the standard and flawed tube with simulated artifact, and terrain plots of the sizing profile near the degraded region of the tube. Eddy current data for each test case involving simulated OD artifact was collected separately, i.e., the entire batch of tubes was scanned each time. Acquisition frequencies represent typical primary and auxiliary channels that are used for the inspection of thin-wall SG tubing.

Figures 4 and 5 show representative NDE profiles of laboratory-grown ODS/CC with and without the simulated OD support structure over the degraded section of the tube. The estimated maximum depth of cracks varied by <10% of tube wall thickness for all of the test cases that were considered. As expected, the effect of OD simulated collars is less significant for larger amplitude signals, and more significant for the smaller amplitude portions of the flaw. For the specimens shown here, NDE flaw depth and length vary within the range that is expected from such factors as probe alignment and data acquisition parameters (i.e., variations in sampling rate, rotational and push/pull speed). Studies so far suggest that the degree of signal distortion depends primarily on the artifact geometry and composition, as well as on signal amplitude at a given excitation frequency.

2.5 Comparison of NDE with Destructive Examination Results

Crack profiles from the destructive analyses (fractography) were compared with those obtained from the multiparameter algorithm. Representative test cases are shown in Fig. 6. Figure 7(a) shows comparison of the maximum depths as determined by fractography and the multiparameter algorithm. A linear regression fit and 95% confidence bounds for the observed data as a function of the multiparameter estimates are also shown in the figure. Because the field of view of the rotating pancake probe is limited, the depth measurements at points ≥ 5 mm apart



(b)

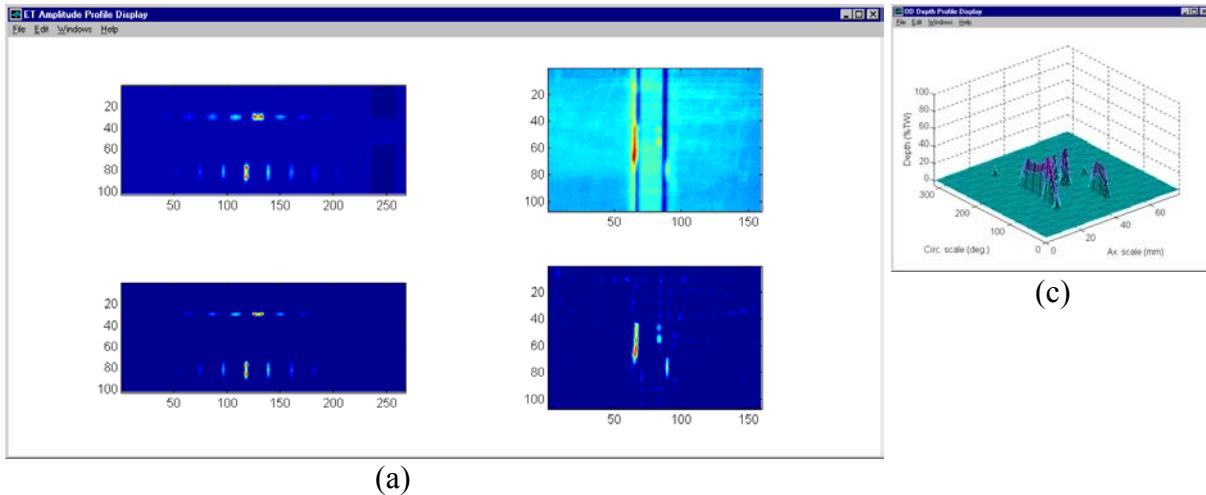


Figure 4. Data analysis results for specimen with laboratory-grown ODSCC, showing (a) image display of scanned region of standard and flawed tube with TSP collar placed over crack. Also shown are terrain plots of depth profile over approximately same region of tube (b) without and (c) with TSP collar. Estimated maximum depth ($<50\%$ TW from plain tube) varies by $<10\%$ TW for all simulated artifacts.

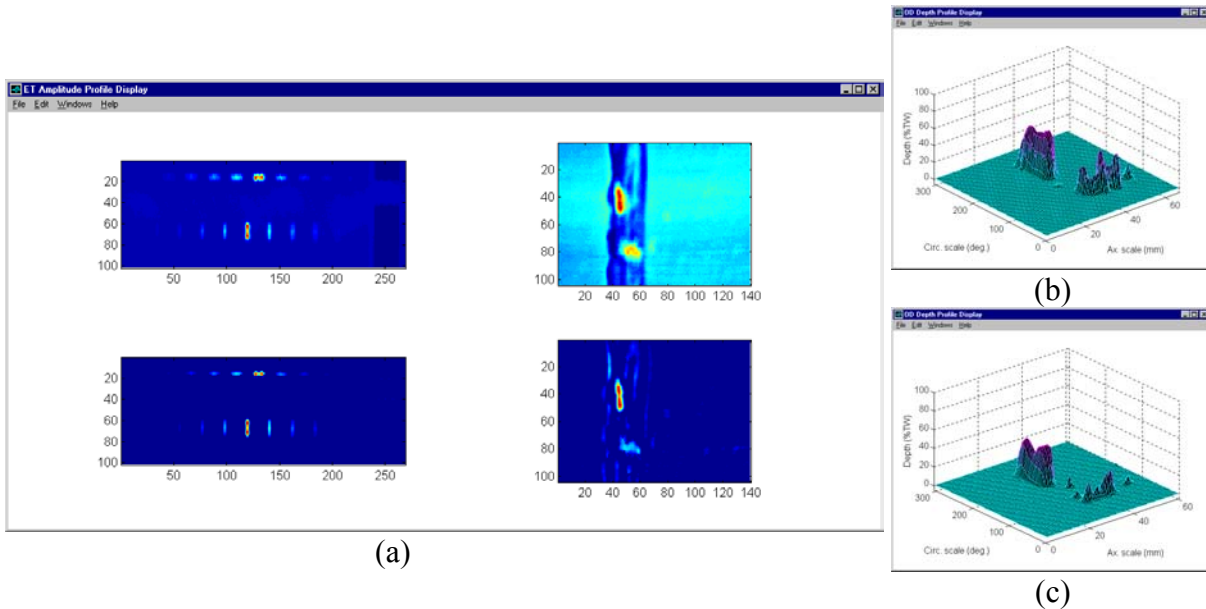


Figure 5. Data analysis results for specimen with laboratory-grown ODSCC, showing (a) image display of scanned region of standard and flawed tube with magnetite collar placed over crack. Also shown are terrain plots of depth profile over approximately same region of tube (b) without and (c) with magnetite collar. Estimated maximum depth ($<50\%$ TW from plain tube) varies by $<10\%$ TW for all simulated artifacts.

along the crack profile are essentially independent; additional comparisons of the estimated depth with that determined by fractography were made at various points along the crack profile. Figure 7(b) shows the results for 89 points from 20 cracks, axial and circumferential, ID and OD;

linear regression curve and 95% confidence bounds for the observed data as a function of the multiparameter estimates are also shown.

3. Conclusion

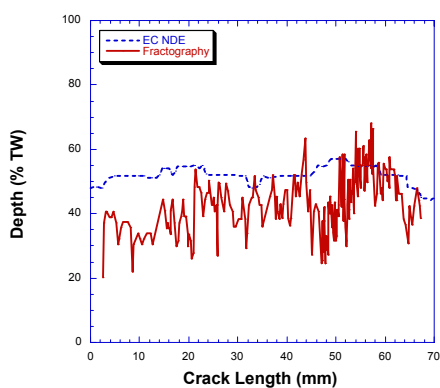
Computer-aided data analysis techniques can provide reliable and efficient processing of multifrequency EC data acquired with high-resolution probes. The basic structure of a data analysis scheme for the processing of EC recordings with a standard rotating probe was described. NDE assessments so far have been limited to analyses of data from rotating pancake coils. Implementation of data conversion, calibration, and analysis routines for off-line manipulation of inspection results was discussed. Selected examples from analyses of laboratory-produced specimens with chemically induced cracking were provided to illustrate the results. Also flaw profiles estimated by NDE were compared with true-state profiles determined by fractography. The influence of undesired signals from support structures and deposits on the sizing results was assessed by analysis of a subset of tubes with simulated artifacts. Through comparative studies, results of these investigations have demonstrated that improved sizing accuracy and efficiency in the processing of data can be achieved by integrating suitable algorithms for computer-aided analysis of EC inspection results.

ACKNOWLEDGMENTS

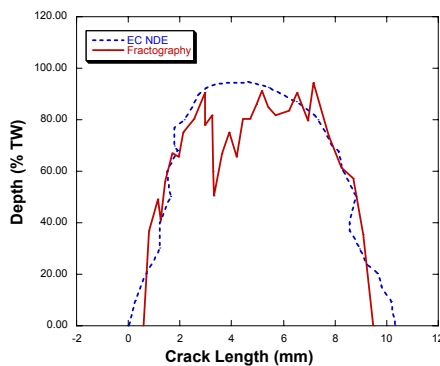
Work sponsored by the Office of Nuclear Regulatory Research, U.S. Nuclear Regulatory Commission, under Job Code W6487.

REFERENCES

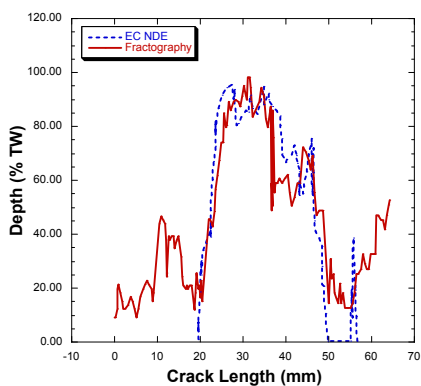
1. S. Bakhtiari and D. S. Kupperman, "Advanced NDE for Steam Generator Tubing," NUREG/CR-6638, U.S. Nuclear Regulatory Commission, Washington, DC, January 2000.
2. S. Bakhtiari, J. Y. Park, D. S. Kupperman, S. Majumdar, and W. J. Shack, "Advanced NDE for Steam Generator Tubing," NUREG/CR-6746, U.S. Nuclear Regulatory Commission, Washington, DC, August 2001.
3. D. R. Diercks, S. Bakhtiari, K. E. Kasza, D. S. Kupperman, S. Majumdar, J. Y. Park, and W. J. Shack, "Steam Generator Tube Integrity Program, Annual Report, October 1999-September 2000," NUREG/CR-6511, Vol. 8, U.S. Nuclear Regulatory Commission, Washington, DC, February 2002.



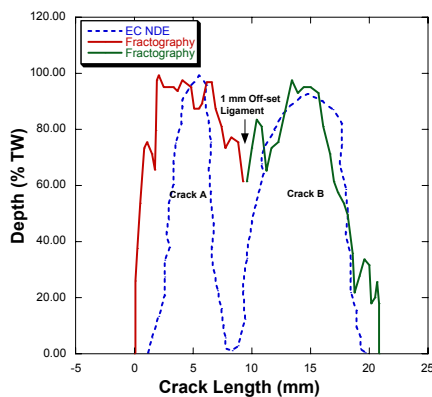
(a)



(b)

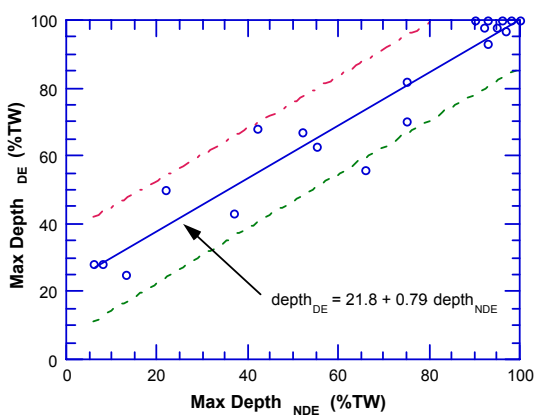


(c)

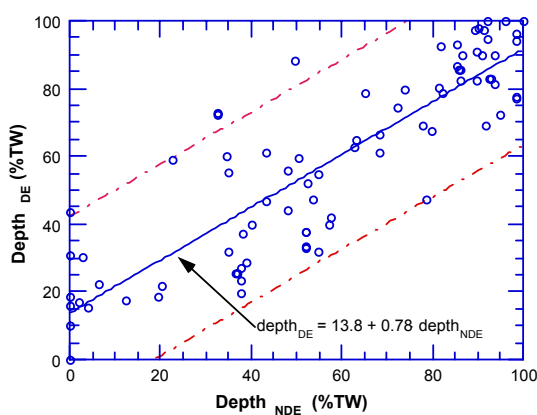


(d)

Figure 6. Comparison of NDE and fractography profiles of representative laboratory-produced specimen with (a) circumferential IDSCC, (b) axial ODSCC, (c) circumferential ODSCC, and (d) axial nonplanar ODSCC.



(a)



(b)

Figure 7. Plots of (a) maximum depth and (b) depth along flaw as determined by fractography vs. NDE estimates. Also shown are regression fit and estimated 95% bounds for observed depth as a function NDE depth estimate.